Group 10 Transition-Metal Complexes of an Ambiphilic PSB-Ligand: Investigations into η^3(*BCC*)-Triarylborane Coordination

David J. H. Emslie,* Laura E. Harrington,† Hilary A. Jenkins,† Craig M. Robertson,† and James F. Britten†

Department of Chemistry, McMaster University, 1280 Main Street West, Hamilton, Ontario L8S 4M1, Canada

Received July 15, 2008

Reaction of 2,7-di-*tert*-butyl-5-diphenylboryl-4-diphenylphosphino-9,9-dimethylthioxanthene (TXPB) with [$PdCl_2$(COD)] resulted in the formation of [PdCl(μ-Cl)(TXPB)] (**3**), which can be reduced in a stepwise fashion, forming [Pd(TXPB)] (**2**) via [{Pd^I(μ-Cl)(TXPB)}$_2$] (**4**). Dinuclear **4** could also be prepared through a comproportionation reaction of palladium(II) complex [PdCl(μ-Cl)(TXPB)] (**3**) with either [Pd(TXPB)] (**2**) or [Pd(dba)(TXPB)] (**5**). In complexes **3** and **4**, the TXPB ligand is bound to palladium via the phosphine and thioether donors, with a chloride anion bridging between the metal and the borane unit of TXPB. By contrast, the TXPB ligand in **2** is bound to palladium not only via the phosphine and thioether donors but also through a Pd-(η^3-BAr_3) linkage involving boron and the *ipso*- and *ortho*-carbon atoms of one *B*-phenyl ring. The analogous nickel complex, [Ni(TXPB)] (**6**) also proved accessible by direct reaction of [Ni(COD)$_2$] with TXPB. In both **2** and **6**, short distances (2.02−2.33 Å) between the metal and the B−C_{ipso}−C_{ortho} unit of TXPB and ^{11}B NMR signals shifted 38−39 ppm to lower frequency of free TXPB confirm the presence of a strong M−{η^3(*BCC*)-BAr_3} interaction. Reaction of either [Pd_2(dvds)$_3$] (dvds = 1,3-divinyltetramethyldisiloxane) with TXPB or complex **2** with dvds resulted in rapid formation of [(κ^1-TXPB)Pd(η^2:η^2-dvds)] (**7**). The platinum analogue of complex **7**, [(κ^1-TXPB)Pt(η^2:η^2-dvds)] (**8**), was also prepared by reaction of [Pt(COD)$_2$] with dvds, followed by TXPB. In both **7** and **8**, the metal is trigonal planar as a result of η^2:η^2-coordination to dvds and bonding only to the phosphine group of TXPB. To assess the potential for a ligand with the same structural characteristics as TXPB to coordinate via three η^1-interactions, the phosphine analogue of TXPB; 2,7-di-*tert*-butyl-4,5-bis(diphenylphosphino)-9,9-dimethylthioxanthene (Thioxantphos) was prepared, and reaction with [PtX_2(COD)] resulted in the clean formation of [PtX(Thioxantphos)]X where X = Cl (**9**) and I (**10**). These complexes are square planar with the Thioxantphos ligand coordinated through three η^1-interactions, confirming the steric accessibility of more traditional κ^3-coordination in 4,5-disubstituted thioxanthene ligands such as Thioxantphos and TXPB.

Introduction

A wide variety of compounds containing transition metal−boron interactions have been reported, including polyhedral borane and carborane complexes,[1] complexes of boron-containing cyclic π-ligands (e.g., anionic boratabenzenes and dianionic boroles),[2] boryl (L_xM-BR_2), borylene ($L_xM{=}BR$), boride, and borane ($L_xM{\rightarrow}BR_3$) complexes,[3,4] borataalkene {$L_xM-(\eta^2$-$R_2BCR_2)$} complexes,[5,6] and metal−(HBR_2) σ-complexes.[7] However, within this group, borane ligands are unique[5,8] as zero-electron (Z-type) ligands which can be considered to act as σ-acceptors with respect to a coordinated metal.[9−11] Besides fundamental studies into the electronic consequences and

* To whom correspondence should be addressed. Phone: 905-525-9140. Fax: 905-522-2509. E-mail: emslied@mcmaster.ca.

† McMaster Analytical X-Ray Diffraction Facility.

(1) (a) Casanova, J. *The borane, carborane, carbocation continuum*; Wiley: New York, 1998. (b) Grimes, R. N. *Metal Interactions with Boron Clusters*; Plenum Press: New York, 1982.

(2) (a) Herberich, G. E.; Ohst, H. *Adv. Organomet. Chem.* **1986**, *25*, 199. (b) Fu, G. C. *Adv. Organomet. Chem.* **2001**, *47*, 101. (c) Herberich, G. E. In *Comprehensive Organometallic Chemistry II*; Abel, E. W., Stone, F. G. A., Wilkinson, G., Ed.; Pergamon Press: Oxford, 1995; Vol. 1, p 197.

(3) (a) Braunschweig, H.; Colling, M. *Coord. Chem. Rev.* **2001**, *223*, 1. (b) Braunschweig, H.; Kollann, C.; Rais, D. *Angew. Chem., Int. Ed.* **2006**, *45*, 5254. (c) Braunschweig, H.; Whittell, G. R. *Chem.—Eur. J.* **2005**, *11*, 6128. (d) Aldridge, S.; Coombs, D. L. *Coord. Chem. Rev.* **2004**, *248*, 535.

(4) Braunschweig, H. *Angew. Chem., Int. Ed.* **1998**, *37*, 1786.

(5) Tantalum borataalkene complexes of the form [Cp_2Ta{CH_2B-(C_6F_5)$_2$}] and [Cp_2TaL{$CH_2B(C_6F_5)_2$}] (L = CO or *t*-BuNC) have been investigated, and the η^2-borataalkene bonding mode has been considered either to mirror the Dewar−Chatt−Duncanson model for olefins or to involve of a covalent Ta−C σ-bond and a metal to boron dative bond. Both olefin-like reactivity and reactivity that likely involves an η^1-coordinated form of the borataalkene ligand have been observed: (a) Cook, K. S.; Piers, W. E.; Rettig, S. J *Organometallics* **1999**, *18*, 1575. (b) Cook, K. S.; Piers, W. E.; Woo, T. K.; McDonald, R. *Organometallics* **2001**, *20*, 3927. (c) Cook, K. S.; Piers, W. E.; McDonald, R. *J. Am. Chem. Soc.* **2002**, *124*, 5411. (d) Cook, K. S.; Piers, W. E.; Hayes, P. G.; Parvez, M. *Organometallics* **2002**, *21*, 2422.

(6) (a) Zhang, S.; Piers, W. E.; Gao, X.; Parvez, M. *J. Am. Chem. Soc.* **2000**, *122*, 5499. (b) Scollard, J. D.; McConville, D. H.; Rettig, S. J. *Organometallics* **1997**, *16*, 1810. (c) Thorn, M. G.; Vilardo, J. S.; Fanwick, P. E.; Rothwell, I. P. *Chem. Commun.* **1998**, 2427.

(7) Kubas, G. J. *J. Organomet. Chem.* **2001**, *635*, 37.

(8) Several complexes containing bridging boryl ligands, which may be considered metal−borane complexes in which one of the borane substituents is a second metal center (Figure 1, complex D) have been reported. See, for example: (a) Reference 35. (b) Westcott, S. A.; Marder, T. B.; Baker, R. T.; Harlow, R. L.; Calabrese, J. C.; Lam, K. C.; Lin, Z. *Polyhedron* **2004**, *23*, 2665. (c) Braunschweig, H.; Radacki, K.; Rais, D.; Whittell, G. R. *Angew. Chem., Int. Ed.* **2005**, *44*, 1192. In parts a and b of this reference, the boryl ligand adopts an unsymmetrical bridging mode, while in part c, approximately symmetrical bridging with near tetrahedral geometry at boron was observed.

10.1021/om800670e CCC: $40.75
Publication on Web 09/18/2008

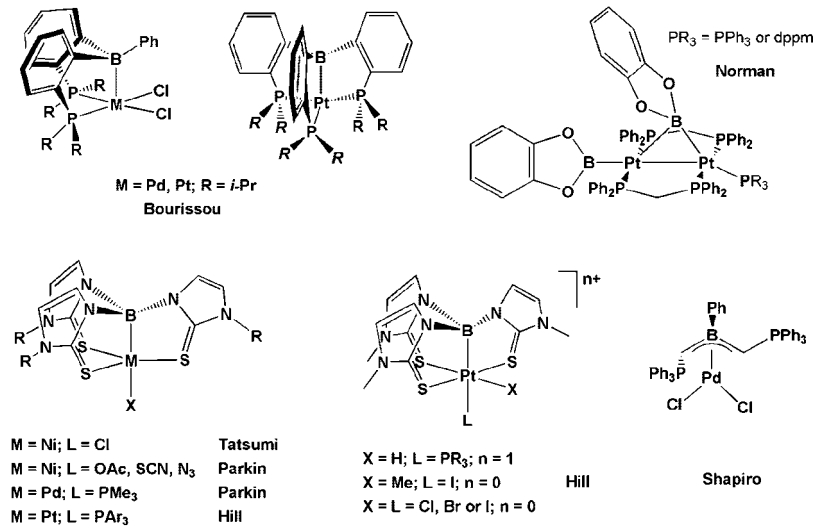

Figure 1. Representative group 10 metal−borane and closely related complexes: A,[32,33] B,[25,27,30,34] C,[21,22,25] D,[35] and E.[36]

metal−ligand interactions involved in metal−borane coordination, metal−borane complexes are also of great interest for the development of new catalytic reactivity: (a) as a direct result of M−BR_3 bonding, which increases the coordination number by one but reduces the d-electron count by two units,[10] often resulting in unusual geometries for a given d-electron configuration, (b) due to the potential for pendant or coordinated borane groups to bind, position and/or activate organic substrates (bifunctional catalysis), and/or (c) as a result of coligand (e.g., Me or Cl) coordination or abstraction.[12−18]

Despite increased current interest in transition metal−borane complexes, they are still scarce, perhaps due to difficulties in the preparation of complexes of this type using boranes that are not incorporated into an ambiphilic (containing one or more Lewis basic donor in addition to the borane) ligand framework, combined with the tendency for potential ambiphilic ligands to form unreactive or insoluble inter- or intramolecular Lewis acid−base adducts.[19] The first well authenticated[4] metal−borane complex, $[CpFe(CO)_2(BPh_3)]^-$, was prepared by Burlitch et al. in 1979.[20] However, a crystallographically characterized metal−borane complex was not reported until 1999 by Hill et al.; $[\{\kappa^4\text{-B(mt)}_3\}Ru(CO)(PPh_3)]$ (mt = *N*-alkylimazolyl).[8] Since then, various $B(mt)_3$ (Figure 1, parts B and C) as well as $RB(mt)_2$ and $B(taz)_3$ (taz = 3,4-dialkyl-5-thioxo-1,2,4-triazolyl) complexes have been reported by Hill (M = Ru, Os, Pt, Rh, Ir)[11,21−25] and Parkin (M = Rh, Ir, Ni, Pd, Fe),[26−28] as well as Connelly, Tatsumi, and Rabinovich (M = Rh, Ni, and Co,

(9) Sircoglou, M.; Bontemps, S.; Mercy, M.; Saffon, N.; Takahashi, M.; Bouhadir, G.; Maron, L.; Bourissou, D. *Angew. Chem., Int. Ed. Engl.* **2007**, *46*, 8583.

(10) Parkin, G. *Organometallics* **2006**, *25*, 4744.

(11) Hill, A. F. *Organometallics* **2006**, *25*, 4741.

(12) Formal 1,2-addition of X_2 or XY across the Fe−BR_3 bond in $[\{\kappa^4\text{-B(mim}^{t\text{Bu}})_3\}Fe(CO)_2]$ has been reported using $(O_2CPh)_2$, $CHCl_3$, $CHBr_3$, or $I_2/CHCl_3$. In addition, reaction of $[\{\kappa^4\text{-B(mim}^{t\text{Bu}})_3\}NiCl]$ with XeF_2 gave $[\{\kappa^3\text{-FB(mim}^{t\text{Bu}})_3\}NiCl]$, while reaction with I_2, $CHBr_3$, or $CHCl_3$ gave $[\{\kappa^3\text{-ClB(mim}^{t\text{Bu}})_3\}NiX]$ (X = I, Br, or Cl), and reaction of $[\{\kappa^4\text{-B(mim}^{t\text{Bu}})_3\}NiX]$ (X = Cl, NCS, or N_3) with I_2 gave $[\{\kappa^3\text{-XB(mim}^{t\text{Bu}})_3\}NiI]$: ref 26.

(13) The reaction of $Na[H_2B(mt)_2]$ with $[RhCl(CS)(PPh_3)_2]$ resulted in formation of $[LRhH(PPh_3)]$ [L = $\{H(mt)_2B\}(Ph_3P)C{=}S$] in which CS has been converted to a zwitterionic $(R_3B)(Ph_3P)C{=}S$ ligand. This reaction is considered to proceed via the intermediate $[\{\kappa^3\text{-HB(mt)}_2\}RhH(CS)(PPh_3)]$: ref 24e.

(14) Reaction of $[(dmpe)NiMe_2]$ with $Ph_2P(CH_2)_2BR_2$ ($BR_2 = BCy_2$ or BBN) resulted in the formation of zwitterionic $[(dmpe)NiMe(\kappa^1\text{-Ph}_2\text{P-(CH}_2)_2BR_2Me)]$ as a result of methyl abstraction by the borane: ref 34.

(15) Reaction of $[Pd_2(dba)_3]$ with TXPB gave [Pd(dba)(TXPB)] (**5**, Scheme 1) which is best regarded as a zwitterionic η^3-boratoxyallyl complex: ref 39.

(16) A substantial rate enhancement has been reported for the dehydrogenative coupling of $PhSiH_3$ by [(Me-Ind)NiMe(PPh$_3$)] in the presence of $Me_2PCH_2AlMe_2$. The proposed intermediate in this reactivity is $[(Me\text{-Ind})NiMe\{Me_2PCH_2AlMe_2\}]$. A related rhodium complex, $[Cp^*RhMe_2\{\kappa^1\text{-Me}_2PCH_2AlMe_2\text{-OSMe}_2\}]$, has also been prepared:(a) Fontaine, F.-G.; Zargarian, D. *J. Am. Chem. Soc.* **2004**, *126*, 8786. (b) Thibault, M.-H.; Boudreau, J.; Mathiotte, S.; Drouin, F.; Sigouin, O.; Michaud, A.; Fontaine, F.-G. *Organometallics* **2007**, *26*, 3807.

(17) Both early and late transition-metal complexes of borane-appended cyclopentadienyl ligands have been reported, and observed reactivity includes electrophilic addition to the adjacent cyclopentadienyl ring and coordination of Lewis bases by the borane, followed in certain cases by C−H bond activation: (a) Herrmann, C.; Kehr, G.; Fröhlich, R.; Erker, G. *Eur. J. Inorg. Chem.* **2008**, 2273. (b) Herrmann, C.; Kehr, G.; Fröhlich, R.; Erker, G. *Organometallics* **2008**, *27*, 2328. (c) Hill, M.; Kehr, G.; Erker, G.; Kataeva, O.; Fröhlich, R. *Chem. Commun.* **2004**, 1020. (d) Hill, M.; Erker, G.; Kehr, G.; Fröhlich, R.; Kataeva, O. *J. Am. Chem. Soc.* **2004**, *126*, 11046. (e) Hill, M.; Kehr, G.; Fröhlich, R.; Erker, G. *Eur. J. Inorg. Chem.* **2003**, 3583.

(18) See refs 40 and 41 for complexes containing M−Cl−BR_3 interactions.

(19) (a) Weis, N.; Pritzkow, H.; Siebert, W. *Eur. J. Inorg. Chem.* **1999**, 7. (b) Görz, D.; Pritzkow, H.; Siebert, W. *Eur. J. Inorg. Chem.* **2003**, 2783. (c) Müller, G.; Lachmann, J. *Z. Naturforsch. B* **1993**, *48*, 1248. (d) Rathke, J.; Schaeffer, R. *Inorg. Chem.* **1972**, *11*, 1150. (e) Sugihara, Y.; Miyatake, R.; Takakura, K.; Yano, S. *Chem. Commun.* **1994**, 1925. (f) Giles, R. L.; Howard, J. A. K.; Patrick, L. G. F.; Probert, M. R.; Smith, G. E.; Whiting, A. *J. Organomet. Chem.* **2003**, *680*, 257. (g) Spies, P.; Fröhlich, R.; Kehr, G.; Erker, G.; Grimme, S. *Chem.—Eur. J.* **2008**, *14*, 333.

(20) $[CpFe(CO)_2(BPh_3)]^-$ was characterized spectroscopically, but an X-ray crystal structure was not obtained. However, X-ray crystal structures for both the the $AlPh_3$ analogue, $[CpFe(CO)_2(AlPh_3)]^-$, and the product of $[CpFe(CO)_2(BPh_3)]^-$ decomposition in THF, $[(Ph_3BC_5H_4)Fe_2(CO)_4\text{-Cp}]^-$, were obtained: (a) Burlitch, J. M.; Burk, J. H.; Leonowicz, M. E.; Hughes, R. E. *Inorg. Chem.* **1979**, *18*, 1702. (b) Burlitch, J. M.; Leonowicz, M. E.; Petersen, R. B.; Hughes, R. E. *Inorg. Chem.* **1979**, *18*, 1097.

(21) Crossley, I. R.; Hill, A. F.; Willis, A. C. *Organometallics* **2008**, *27*, 312.

(22) Crossley, I. R.; Hill, A. F. *Dalton Trans.* **2008**, 201.

(23) (a) Crossley, I. R.; Hill, A. F.; Willis, A. C. *Organometallics* **2006**, *25*, 289. (b) Crossley, I. R.; Hill, A. F.; Humphrey, E. R.; Willis, A. C. *Organometallics* **2005**, *24*, 4083. (c) Crossley, I. R.; Foreman, M. R.; St, J.; Hill, A. F.; White, A. J. P.; Williams, D. J. *Chem. Commun.* **2005**, 221.

(24) (a) Crossley, I. R.; Hill, A. F.; Willis, A. C. *Organometallics* **2005**, *24*, 4889. (b) Crossley, I. R.; Hill, A. F.; Willis, A. C. *Organometallics* **2005**, *24*, 1062. (c) Foreman, M. R; St, J.; Hill, A. F.; White, A. J. P.; Williams, D. J. *Organometallics* **2004**, *23*, 913. (d) Foreman, M. R. St.-J.; Hill, A. F.; Owen, G. R.; White, A. J. P.; Williams, D. J. *Organometallics* **2003**, *22*, 4446. (e) Crossley, I. R.; Hill, A. F.; Willis, A. C. *Organometallics* **2007**, *26*, 3891. (f) Crossley, I. R.; Foreman, M.; Hill, A. F.; Owen, G. R.; White, A. J. P.; Williams, D. J.; Willis, A. C. *Organometallics* **2008**, *27*, 381.

(25) Crossley, I. R.; Hill, A. F. *Organometallics* **2004**, *23*, 5656.

respectively).[29−31] All of these complexes were prepared starting from anionic $HB(mt)_3$, $HBR(mt)_2$, or $HB(taz)_3$ ligands, with the borane ligand formed through various processes, including H-migration from boron to a coordinated metal or formal elimination of HR, HX, or H^+ from an initial precursor complex.

In contrast to the ambiphilic ligands described above, which are generated in situ at a coordinated metal, several free ambiphilic triarylborane-containing ligands $Ph_{(3-n)}B\{C_6H_4(PR_2)\text{-}o\}_n$ (R = *i*-Pr or Ph; *n* = 2 or 3) and $FluB\{C_6H_4(P\text{-}i\text{-}Pr_2)\text{-}o\}$ (BFlu = borafluorenyl) were recently reported (2006−2008) by Bourissou et al. and successfully deployed for the formation of metal−borane complexes with Rh, Pd, Pt, and Au (Figure 1A).[9,32,33,37,38] In 2006, we also reported a free ambiphilic ligand; a phosphine−thioether−borane ligand based on the rigid thioxanthene backbone (TXPB; Scheme 1).[39] Reaction of TXPB with $0.5[Rh(\mu\text{-}Cl)(CO)_2\}_2]$ gave $[(TXPB)Rh(\mu\text{-}Cl)(CO)]$ in which the borane engages in a Rh−Cl−BR_3 bridging interaction, and subsequent reaction with $K[CpFe(CO)_2]$ resulted in chloride substitution to form heterobimetallic $[(TXPB)Rh(\mu\text{-}CO)_2Fe(CO)\text{-}Cp]$ (**1**). The X-ray crystal structure of **1** revealed the presence of a unique M−(η^3-BAr_3) interaction (M = Rh) involving boron and the *ipso*- and *ortho*-carbon atoms on one *B*-phenyl ring (Scheme 1), rather than a more typical M−(η^1-BAr_3) interaction.[40] An interaction of this type between a vinyl- or arylborane and a metal had not previously been reported, and intriguingly, only M−(η^1-BAr_3) interactions have been observed in the metal−triarylborane complexes reported by Bourissou.

Although in complex **1**, close approach of the B−C_{ipso}−C_{ortho} unit to the metal could perhaps be attributed to the presence only of an η^2-interaction between rhodium and one *B*-phenyl ring, or considered simply a consequence of the rigidity of the TXPB ligand, a significant Rh−{η^3(*BCC*)-BAr_3} interaction was proposed on basis of DFT calculations, a substantial upfield shift of the ^{11}B NMR signal relative to that of the free ligand, Rh−B, Rh−C_{ipso}, and Rh−C_{ortho} distances of 2.63(2), 1.97(2), and 2.03(2) Å, respectively, and a relatively short P···B distance [4.77(2) Å]. DFT calculations also highlighted the presence of significant delocalization within the η^3-coordinated BCC unit to the extent that for **1**, the most appropriate bonding description is intermediate between that expected for an isolated borane/alkene complex and a fully delocalized allyl-like complex. However, the Rh−B distance in **1** is substantially longer than Rh−B in related Rh−(η^1-BR_3) complexes (2.09−2.35 Å),[23,28,29,32,37] and low quality X-ray crystallographic data and the bimetallic nature of **1** complicated further analysis in this system.[40] Herein, we describe the synthesis and reactivity of mononuclear and monoligated [Pd(TXPB)] (**2**) and [Ni(TXPB)] (**6**) which contain M−{η^3(*BCC*)-BAr_3} interactions with metal−boron distances

Scheme 1. Preparation of Complexes 2−5[a]

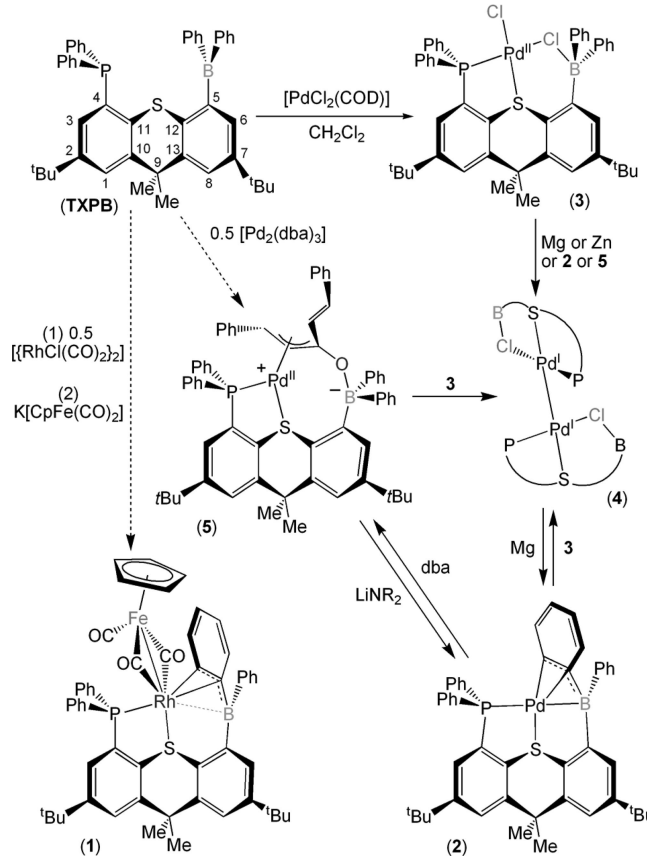

[a] Dashed arrows indicate previously reported reactivity.

Scheme 2. Preparation of Complexes 6−8

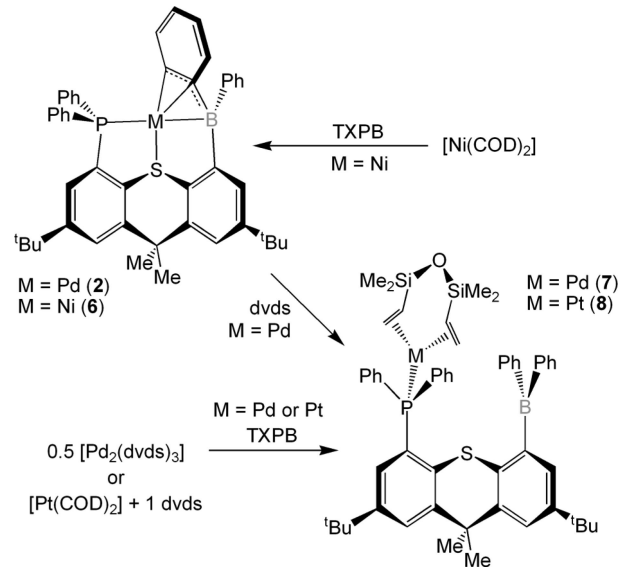

(26) (a) Pang, K.; Tanski, J. M.; Parkin, G. *Chem. Commun.* **2008**, 1008. (b) Figueroa, J. S.; Melnick, J. G.; Parkin, G. *Inorg. Chem.* **2006**, *45*, 7056.
(27) Pang, K.; Quan, S. M.; Parkin, G. *Chem. Commun.* **2006**, 5015.
(28) Landry, V. K.; Melnick, J. G.; Buccella, D.; Pang, K.; Ulichny, J. C.; Parkin, G. *Inorg. Chem.* **2006**, *45*, 2588.
(29) Blagg, R. J.; Charmant, J. P. H.; Connelly, N. G.; Haddow, M. F.; Orpen, A. G. *Chem. Commun.* **2006**, 2350.
(30) Senda, S.; Ohki, Y.; Hirayama, T.; Toda, D.; Chen, J.-L.; Matsumoto, T.; Kawaguchi, H.; Tatsumi, K. *Inorg. Chem.* **2006**, *45*, 9914.
(31) Mihalcik, D. J.; White, J. L.; Tanski, J. M.; Zakharov, L. N.; Yap, G. P. A.; Incarvito, C. D.; Rheingold, A. L.; Rabinovich, D. *Dalton Trans.* **2004**, 1626.
(32) Bontemps, S.; Sircoglou, M.; Bouhadir, G.; Puschmann, H.; Howard, J. A. K.; Dyer, P. W.; Miqueu, K.; Bourissou, D. *Chem.—Eur. J.* **2008**, *14*, 731.
(33) Bontemps, S.; Bouhadir, G.; Gu, W.; Mercy, M.; Chen, C.-H.; Foxman, B. M.; Maron, L.; Ozerov, O. V.; Bourissou, D. *Angew. Chem., Int. Ed.* **2008**, *47*, 1481.
(34) Fischbach, A.; Bazinet, P. R.; Waterman, R.; Tilley, T. D. *Organometallics* **2008**, *27*, 1135.
(35) Curtis, D.; Lesley, M. J. G.; Norman, N. C.; Orpen, A. G.; Starbuck, J. *Dalton Trans.* **1999**, 1687.
(36) Jiang, F.; Shapiro, P. J.; Fahs, F.; Twamley, B. *Angew. Chem., Int. Ed.* **2003**, *42*, 2651.
(37) Bontemps, S.; Gornitzka, H.; Bouhadir, G.; Miqueu, K.; Bourissou, D. *Angew. Chem., Int. Ed.* **2006**, *45*, 1611.
(38) Bontemps, S.; Bouhadir, G.; Miqueu, K.; Bourissou, D. *J. Am. Chem. Soc.* **2006**, *128*, 12056.
(39) Emslie, D. J. H.; Blackwell, J. M.; Britten, J. F.; Harrington, L. E. *Organometallics* **2006**, *25*, 2412.
(40) Oakley, S. R.; Parker, K. D.; Emslie, D. J. H.; Vargas-Baca, I.; Robertson, C. M.; Harrington, L. E.; Britten, J. F. *Organometallics* **2006**, *25*, 5835.

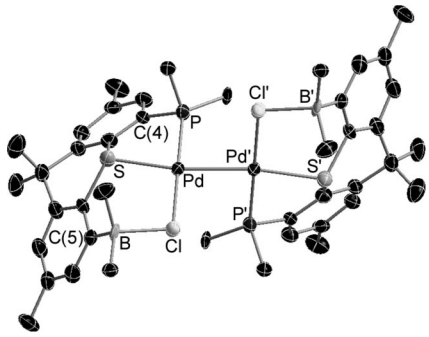

Figure 2. ORTEP of **4**·hexane with solvent, hydrogen atoms, C*Me*$_3$ groups, and the ortho, meta, and para carbon atoms of all unsubstituted phenyl rings omitted for clarity (50% thermal ellipsoids). Selected bond lengths (Å) and angles (deg): Pd−P 2.197(2), Pd−S 2.382(2), Pd−Cl 2.362(2), Pd−Pd′ 2.530(1), B−Cl 1.981(8), P···B 5.391(8), P−Pd−S 83.13(7), S−Pd−Cl 97.22(6), Cl−Pd−Pd′ 93.78(5), P−Pd−Pd′ 85.93(6), P−Pd−Cl 178.14(7), S−Pd−Pd′ 168.84(5), Pd−Cl−B 104.0(2), Cl−B−C(42) 106.4(4), Cl−B−C(36) 106.9(5), Cl−B−C(5) 107.0(5), C(5)−B−C(36) 113.5(6), C(5)−B−C(42) 113.7(6), C(36)−B−C(42) 108.9(5), ligand bend 39.63(28) [ligand bend = angle between the planes of the C(4) ring and the C(5) ring].

much more comparable to those observed in group 10 M−(η^1-BR_3) complexes. We also report synthesis of palladium and platinum complexes containing a free pendant borane (**7** and **8**) and square-planar [PtX(κ^3-Thixantphos)]X [X = Cl (**9**); I (**10**); Thioxantphos = the phosphine analogue of TXPB (a PSP-donor)] complexes which highlight the steric accessibility of a more traditional κ^3-bonding mode [involving M−(η^1-BAr_3) coordination] for the TXPB ligand.

Results and Discussion

Reaction of the TXPB ligand with [$PdCl_2$(COD)] gave orange [PdCl(μ-Cl)(TXPB)] (**3**) in 87% isolated yield. Complex **3** was characterized by NMR spectroscopy (^{31}P δ 58 ppm; ^{11}B δ 13 ppm) and elemental analysis, and by analogy with related [Rh(μ-Cl)(CO)(TXPB)][40] and complex **4** (vide infra), the structure of **3** can be considered to be square planar with one chloride anion bridging between palladium and the borane unit of TXPB (Scheme 1).[41]

The cyclic voltammogram (CV) of **3** in THF showed an irreversible reduction at E_{pc} = −0.94 V vs SCE (ν = 200 mV s^{-1}) followed by additional reduction peaks at E_{pc} = −2.55 and −2.75 V. The first reduction peak at −0.94 V is associated with an irreversible product peak at E_{pa} = 0.39 V. Addition of Zn powder, Mg powder, or [$CoCp_2$] to **3** resulted in the formation of a new bright orange-red product: [{Pd^I(μ-Cl)(TXPB)}$_2$] (**4**; Scheme 1).

The solid-state structure revealed that **4** (Figure 2; Table 1) is a rare example of a neutral palladium(I) dimer containing an unsupported Pd−Pd bond [2.530(1) Å].[42] The TXPB ligand is *P*,*S*-coordinated to palladium(I) with the chloride anion bridging between palladium and the borane unit of TXPB. The geometry at boron approaches tetrahedral [Σ(C−B−C) = 336.1(10)°], while the palladium centers are distorted square planar [Pd−Pd′−S = 168.84(5)°] with an angle of 67° between the two coordination planes. Preservation of a strong interaction between the borane and the chloride ligand in solution is confirmed by an ^{11}B NMR chemical shift of 2 ppm. Complex **4** can also be prepared through a comproportionation reaction between palladium(II) complex **3** and either of complexes **2** or **5** (vide infra).

Reaction of **3** or **4** with excess Zn, Mg, or [$CoCp_2$] resulted in the formation of a new yellow-orange product, [Pd(TXPB)] (**2**; Scheme 1).[43] ^{1}H and ^{31}P NMR spectra showed that complex **2** is also produced in high yield via the reaction of [Pd(dba)(TXPB)] (**5**) with $LiNEt_2$ or $LiN(SiMe_3)_2$. We were unable to determine the fate of the dba molecule in this reaction, but it clearly does not remain intact since **2** reacts rapidly with dba to reform complex **5** (Scheme 1).

The peak at 18 ppm in the ^{31}P NMR spectrum of **2** confirms palladium coordination by the TXPB ligand, and the ^{11}B NMR chemical shift at 31 ppm is indicative of 4-coordinate boron (cf. 69 ppm in free TXPB). The solid-state structure of **2** (Figure 3, Table 1) reveals that the TXPB ligand is bound to palladium not only via the phosphine and thioether donors but also through a Pd−{η^3(*BCC*)-BAr_3} linkage involving the *ipso*- and *ortho*-carbon atoms of one *B*-phenyl ring.

While the solid-state structures of **1** and **2** reveal a qualitatively similar M−{η^3(*BCC*)-BAr_3} bonding mode with approximate trigonal planarity at boron,[44] complex **2** exhibits a substantially shorter M−B distance [2.320(5) vs 2.63(2) Å]. The M−C_{ipso}, M−C_{ortho}, and P···B distances in **2** are also shorter than those observed in **1** [M−C_{ipso} = 2.198(4) vs 2.33(2) Å; M−C_{ortho} = 2.325(4) vs 2.46(2) Å; P···B = 4.605(5) vs 4.77(2) Å], indicative of notably stronger M−{η^3(*BCC*)-BAr_3} bonding in complex **2**, relative to complex **1**, presumably as a result of reduced steric congestion and increased electron density at the metal. These data, in combination with the ^{11}B NMR chemical shift, indicate that the Pd−{η^3(*BCC*)-BAr_3} interaction is electronic in origin and that close Pd−B approach is due to a bonding interaction between palladium and boron, rather than sterically imposed as a result of an η^2-interaction between palladium and a *B*-phenyl ring.

The M−B distance in **2** is comparable to those in related palladium and platinum $Ph_{(3-n)}B\{C_6H_4(P\text{-}i\text{-}Pr_2)\text{-}o\}_n$ (n = 2 or 3) complexes (2.22−2.65 Å)[32,33] but is longer than those in Pd and Pt tris(*N*-alkylimazolyl)borane complexes (2.05−2.16 Å).[21,27] The M−B bond distance in **2** also approaches that of 2.200(5) Å observed in Shapiro's [$PdCl_2${η^3-PhB($CHPPh_3$)$_2$}] (Figure 1), which is described as a palladium(II) complex of an η^3-coordinated zwitterionic boron-bridged diylide ligand.[36]

The analogous nickel complex, brick-red [Ni(TXPB)] (**6**), also proved accessible through direct reaction of [$Ni(COD)_2$] with

(41) For other examples of metal-chloride-borane bridging interactions, see: (a) Vergnaud, J.; Ayed, T.; Hussein, K.; Vendier, L.; Grellier, M.; Bouhadir, G.; Barthelat, J. C.; Sabo-Etienne, S.; Bourissou, D. *Dalton Trans.* **2007**, 2370. (b) Reference 38. (c) Crevier, T. J.; Bennett, B. K.; Soper, J. D.; Bowman, J. A.; Dehestani, A.; Hrovat, D. A.; Lovell, S.; Kaminsky, W.; Mayer, J. M. *J. Am. Chem. Soc.* **2001**, *123*, 1059. (d) Lancaster, S. J.; Al-Benna, S.; Thornton-Pett, M.; Bochmann, M. *Organometallics* **2000**, *19*, 1599.

(42) (a) Rutherford, N. M.; Olmstead, M. M.; Balch, A. L. *Inorg. Chem.* **1984**, *23*, 2833. (b) Schwalbe, M.; Walther, D.; Schreer, H.; Langer, J.; Görls, H. *J. Organomet. Chem.* **2006**, *691*, 4868. (c) Yi, J.; Miyabayashi, T.; Ohashi, M.; Yamagata, T.; Mashima, K. *Inorg. Chem.* **2004**, *43*, 6596. (d) Vicente, J.; Abad, J.-A.; Martínez-Viviente, E.; Jones, P. G. *Organometallics* **2002**, *21*, 4454. (e) Suzuki, T.; Kashiwabara, K.; Fujita, J. *Bull. Chem. Soc. Jpn.* **1995**, *68*, 1619. (f) Yamamoto, Y.; Yamazaki, H. *Bull. Chem. Soc. Jpn.* **1985**, *58*, 1843.

(43) It is worth noting that formation of a complex containing a bridging metal−halide−borane interaction, followed by reduction to simultaneously remove halides and increase the nucleophilicity of the metal center, represents a new and potentially very versatile approach to the synthesis of low-valent metal−borane complexes.

(44) In complexes **1**, **2**, and **6**, η^3(*BCC*)-triarylborane coordination involves the *B*-phenyl ring oriented into the fold of the TXPB ligand backbone. However, in complex **1**, rhodium is bound to the ortho carbon positioned closest to C(5), whereas in complexes **2** and **6**, the metal is bound to the ortho carbon positioned furthest from C(5) (see Scheme 1).

Table 1. Crystallographic Data Collection and Refinement Parameters for Complexes 4, 2, 6, 7, and 10[a]

structure	**2**·toluene	**4**·hexane	**6**·2hexane	**7**·2hexane	**10**·1.74CH_2Cl_2
formula	$C_{54}H_{56}BPPdS$	$C_{100}H_{110}B_2Cl_2P_2Pd_2S_2$	$C_{59}H_{76}BNiPS$	$C_{61}H_{80}B$ $OPPdSSi_2$	$C_{48.74}H_{51.48}Cl_{3.48}I_2P_2PtS$
formula wt	885.23	1743.26	917.75	1065.67	1303.52
T (K)	173(2)	173(2)	173(2)	100(2)	173(2)
cryst syst	monoclinic	monoclinic	triclinic	monoclinic	triclinic
space group	$P2(1)/n$	$C2/c$	$P\bar{1}$	$P2(1)/n$	$P\bar{1}$
a (Å)	15.9022(16)	31.3273(12)	11.3711(18)	17.160(7)	9.8451(4)
b (Å)	12.5955(13)	14.7189(6)	13.090(2)	9.849(4)	15.2773(8)
c (Å)	23.306(3)	21.3425(8)	16.842(4)	36.227(16)	17.2635(9)
α (deg)	90	90	106.206(5)	90	84.9360(10)
β (deg)	102.427(2)	91.473(2)	97.013(5)	96.351(7)	84.0330(10)
γ (deg)	90	90	106.216(4)	90	89.1790(10)
volume (Å^3)	4558.7(9)	9837.8(7)	2256.5(7)	6085(5)	2572.4(2)
Z	4	4	2	4	2
density (calcd; mg/m^3)	1.290	1.177	1.351	1.163	1.683
μ (mm^{-1})	0.523	0.536	0.553	0.441	4.242
F(000)	1848	3632	988	2256	1266
crystal size (mm^3)	0.20 × 0.10 × 0.02	0.30 × 0.18 × 0.04	0.40 × 0.30 × 0.02	0.49 × 0.17 × 0.04	0.34 × 0.18 × 0.02
θ range for collection (deg)	1.79−28.35	1.30−26.49	2.11−28.28	1.96−22.50	1.34−30.62
no. of reflns collected	59472	40938	28080	47990	38565
no. of indep reflns	11361	10198	11009	7967	15429
completeness to θ max (%)	99.7	100.0	98.1	100.0	97.3
absorption correction	analytical	none	numerical	none	numerical
max and min transmission	1.0 and 0.83	0.98 and 0.81	1.000 and 0.818	0.9826 and 0.8115	1.000 and 0.838
GOF on F^2	1.042	0.925	0.861	1.052	1.022
final R_1 [$I > 2\sigma(I)$] (%)	5.67	7.54	5.67	10.53	5.82

[a] For all complexes: wavelength = 0.71073 Å, and refinement method = full-matrix least-squares on F^2.

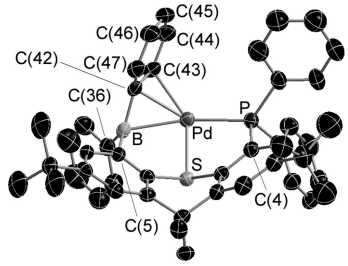

Figure 3. ORTEP of **2**·toluene with solvent, hydrogen atoms, and one orientation of a rotationally disordered CMe_3 group omitted for clarity (50% thermal ellipsoids). Selected bond lengths (Å) and angles (deg): Pd−B 2.320(5), Pd−C(42) 2.198(4), Pd−C(43) 2.325(4), Pd−P 2.343(1), Pd−S 2.316(1), B−C(42) 1.552(6), B−C(36) 1.579(7), B−C(5) 1.611(6), C(42)−C(43) 1.421(6), C(43)−C(44) 1.402(6), C(44)−C(45) 1.366(6), C(45)−C(46) 1.394(7), C(46)−C(47) 1.368(6), C(42)−C(47) 1.432(6), P···B 4.605(5), Pd−cent 1.99, P−Pd−S 85.04(4), S−Pd−B 79.67(12), P−Pd−B 162.02(12), S−Pd−cent 114.2, P−Pd−cent 154.9, ligand bend 54.48(13) [cent = centroid of B, C(42) and C(43); ligand bend = angle between the planes of the C(4) ring and the C(5) ring].

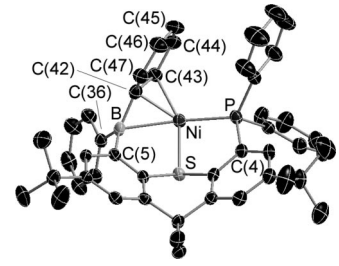

Figure 4. ORTEP of **6**·2hexane with hydrogen atoms and solvent omitted for clarity (50% thermal ellipsoids). Selected bond lengths (Å) and angles (deg): Ni−B 2.297(4), Ni−C(42) 2.019(3), Ni−C(43) 2.081(3), Ni−P 2.190(1), Ni−S 2.1196(8), B−C(42) 1.543(5), B−C(36) 1.591(5), B−C(5) 1.618(4), C(42)−C(43) 1.453(4), C(43)−C(44) 1.412(4), C(44)−C(45) 1.372(5), C(45)−C(46) 1.397(4), C(46)−C(47) 1.439(4), C(42)−C(47) 1.374(4), P···B 4.449(7), Ni−cent = 1.82, P−Ni−S 90.41(3), S−Ni−B 80.87(9), P−Ni−B 164.04(8), S−Ni−cent 116.3, P−Ni−cent 147.7, ligand bend 52.19(14) [cent = centroid of B, C(42) and C(43); ligand bend = angle between the planes of the C(4) ring and the C(5) ring].

TXPB. The structure of **6** is similar to that of **2**, as determined by ^{31}P and ^{11}B NMR spectroscopy (δ 33.9 and 30 ppm, respectively) and X-ray crystallography (Figure 4, Table 1). However, while the M−B distance of 2.297(4) Å is similar, albeit somewhat shorter than that observed in **2** [2.320(5) Å], the Ni−C_{ipso}, Ni−C_{ortho}, and P···B distances of 2.019(3), 2.081(3), and 4.449(7) Å reveal closer approach of the C_{ipso}−C_{ortho} unit to the metal, relative to boron, leading to a less symmetrical η^3-bonding mode in complex **6**. As with **2** and complexes of $Ph_{(3-n)}B\{C_6H_4(P\text{-}i\text{-}Pr_2)\text{-}o\}_n$ ($n = 2-3$),[32,33,37] the M−B bond distance in **6** is somewhat longer than those observed in related M−(η^1-BR_3) complexes of tris(*N*-alkylimazolyl)borane ligands (2.08−2.11 Å for M = Ni).[30,34]

Attempted direct preparation of **2** from the reaction of [Pd_2(dvds)$_3$] (dvds = 1,3-divinyltetramethyldisiloxane) with TXPB resulted in rapid formation of a new product; [(κ^1-TXPB)Pd(η^2:η^2-dvds)] (**7**). This same product was also accessible by reaction of **2** with dvds. Complex **7** has an ^{11}B NMR chemical shift of 74 ppm (cf. 69 ppm for free TXPB), indicative of a 3-coordinate borane, and a ^{31}P NMR chemical shift of 23.7 ppm, illustrating maintained phosphine coordination to palladium. The ^{1}H NMR spectrum of **7** is consistent with a C_s symmetric compound at temperatures between 40 and −80 °C (equivalent vinyl groups of the dvds ligand, but inequivalent methyl groups on silicon), although some dissociation of dvds to reform complex **2** (up to 5% at 40 °C; slow on the NMR time scale) is observed in toluene-d_8 at temperatures above −40 °C. X-ray quality crystals of **7**·2hexane were grown from hexane at −30 °C and confirm a structure in which palladium is approximately trigonal planar as a result of η^2:η^2-coordination to dvds and bonding only to the phosphine group of TXPB (Figure 5, Table 1; despite a high R factor, the structure of **7**·2hexane is suitable to establish connectivity and geometry). The geometry at boron is trigonal planar, and the thioxanthene

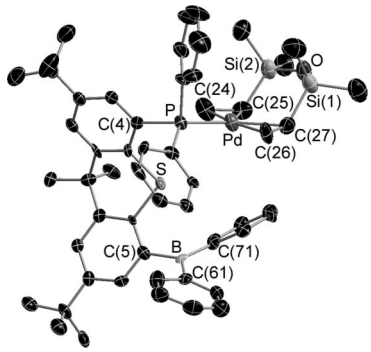

Figure 5. ORTEP of **7**·2hexane with hydrogen atoms and solvent omitted for clarity (50% thermal ellipsoids). Selected bond lengths (Å) and angles (deg): Pd−P 2.308(3), Pd−C(24) 2.180(12), Pd−C(25) 2.171(11), Pd−C(26) 2.148(11), Pd−C(27) 2.188(12), P···B 5.273(12), C(5)−B-C(61) 119.6(9), C(5)−B−C(71) 118.6(10), C(61)−B−C(71) 121.8(9), P−Pd−X 113.47, P−Pd−Y 114.55, X−Pd−Y 131.66, ligand bend 45.85(36) [X = centroid of C(24)/C(25); Y = centroid of C(26)/C(27); ligand bend = angle between the planes of the C(4) ring and the C(5) ring].

backbone of TXPB adopts the characteristic butterfly structure observed in complexes **1**−**6**.

The platinum analogue of complex **7**, [(κ^1-TXPB)Pt(η^2:η^2-dvds)] (**8**), was also prepared by reaction of [Pt(COD)$_2$] with dvds, followed by TXPB.[45] The ^{1}H and ^{13}C NMR spectra of **8** are extremely similar to those of **7**, except that no dvds dissociation is observed, and the vinyl protons and carbon atoms show ^{195}Pt satellites and are shifted to lower frequency.[46] The ^{31}P NMR signal for **8** is located at 21.1 ppm ($^1J_{Pt,P}$ 3661 Hz), and the ^{11}B chemical shift for complex **8** is identical to that of **7** (74 ppm).

The observation of M−{η^3(*BCC*)-BAr$_3$} bonding in **1**, **2**, and **6** lies in stark contrast to the M−(η^1-BAr$_3$) bonding mode observed in the arylborane complexes [{(κ^3-L)Rh(μ-Cl)}$_2$], *cis*-[(κ^3-L)RhCl(DMAP)],[37] *trans*-[(κ^3-L)RhCl(CO)], *cis*-[(κ^3-L)-MCl$_2$] (M = Pd or Pt),[32] [(κ^3-L)AuCl],[9] and [(κ^2-L′)AuCl][38] (L = PhB{C$_6$H$_4$(PR$_2$)-*o*}$_2$; R = *i*-Pr or Ph; L′ = FluB{C$_6$H$_4$-(P-*i*-Pr$_2$)-*o*}; FluB = borafluorenyl) reported recently by Bourissou et al. Analogous M−{η^3(*BCC*)-BAr$_3$} bonding should be sterically accessible with these ligands, bearing in mind that M−(η^3-BAr$_3$) bonding in **1**, **2**, and **6** is characterized by approximate trigonal planarity at boron.[47] Therefore, so long as the coordination environment of the TXPB ligand does not in fact preclude M−(η^1-BAr$_3$) bonding on steric grounds, the preference for η^3-bonding in our system can reasonably be attributed to complexation with more electron rich and coordinatively unsaturated (with respect to typical coordination numbers for a given d-electron configuration) metal fragments. To assess the potential for a ligand with the same structural characteristics as TXPB to coordinate via three η^1-interactions, we prepared the phosphine analogue of TXPB; 2,7-di-*tert*-butyl-4,5-bis(diphenylphosphino)-9,9-dimethylthioxanthene (Thioxantphos; ^{31}P δ −10 ppm).[48] This ligand was accessible in 67% yield by dilithiation of TXBr$_2$ followed by reaction with 2 equiv of ClPPh$_2$ (Scheme 3), and is the sulfur analogue of the popular Xantphos ligand pioneered by van Leeuwen et al.

Scheme 3. Preparation and Complexation of Thioxantphos

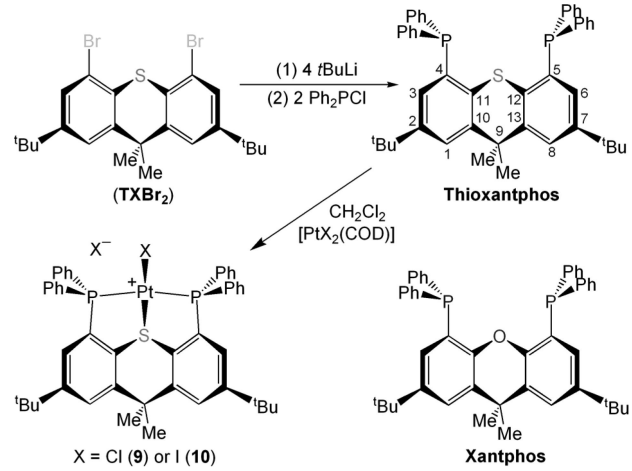

Reaction of Thioxantphos with [PtX$_2$(COD)] (X = Cl and I) resulted in the clean formation of [PtX(Thioxantphos)]X [X = Cl (**9**) and I (**10**); Scheme 3] with very similar ^{1}H and ^{13}C NMR spectra and ^{31}P NMR chemical shifts of 41 ppm ($^1J_{P,Pt}$ 2429 Hz) and 39 ppm ($^1J_{P,Pt}$ 2383 Hz), respectively.[49] Observation of a single ^{31}P NMR signal for **9** and **10**, inequivalent C*Me*$_2$ groups, and insolubility in toluene indicate symmetrical binding of Thioxantphos via both phosphine donors, a bent ligand backbone, and iodide displacement by the thioether donor of Thioxantphos. The solid-state structure of complex **10** (Figure 6; Table 1) confirms that the Thioxantphos ligand is κ^3-coordinated to form a square-planar platinum cation with an iodide counteranion[50,51] and that the thioxanthene backbone of the ligand adopts a butterfly conformation, as is observed for complexes of TXPB. The Pt−S bond distance in **10** is 2.252(2) Å, while the Pt−P bond lengths are 2.318(2) and 2.310(2) Å.[52] These bonds are slightly shorter than Pd−S and Pd−P in complex **2** [2.316(1) and 2.343(1) Å respectively], perhaps due to the cationic nature of **10**. The κ^3-coordination mode observed

(45) [Pt(nb)$_3$] and [Pt(COD)$_2$] react with TXPB to form a mixture of products.

(46) Krause, J.; Cestaric, G.; Haack, K.-J.; Seevogel, K.; Storm, W.; Pörschke, K.-R. *J. Am. Chem. Soc.* **1999**, *121*, 9807.

(47) The complexes [(κ^4-L)Pt] and [(κ^4-L)AuCl] (L = B{C$_6$H$_4$(P-*i*-Pr$_2$)-*o*}$_3$) have also been reported. However, for these complexes, metal−aryl interactions are precluded by κ^4-bonding which aligns all *B*-aryl rings approximately side-on with respect to the metal; see ref 33.

(48) The coordination behavior of a *t*-Bu-free version of Thioxantphos is mentioned in the following paper: Zuideveld, M. A.; Swennenhuis, B. H. G.; Boele, M. D. K.; Guari, Y.; van Strijdonck, G. P. F.; Reek, J. N. H.; Kamer, P. C. J.; Goubitz, K.; Fraanje, J.; Lutz, M.; Spek, A. L.; van Leeuwen, P. W. N. M *Dalton Trans.* **2002**, 2308. However, to the best of our knowledge, a preparation for this ligand has not been published, and it has not been mentioned in any subsequent publications.

(49) The magnitudes of $^1J_{195Pt,31P}$ coupling constants in square planar platinum(II) complexes are known to be very sensitive to the nature of the ligand in the trans position and the overall charge on the complex. See, for example: (a) Pidcock, A.; Richards, R. E.; Venanzi, L. M. *J. Chem. Soc. A* **1966**, 1707. (b) Krevor, J. V. Z.; Simonis, U.; Richter, J. A. *Inorg. Chem.* **1992**, *31*, 2409.

(50) The ionic nature of **9** and **10** is consistent with their insolubility in toluene.

(51) For discussion of analogous platinum complexes of the S(CH$_2$CH$_2$PPh$_2$)$_2$ ligand, see: (a) Andreasen, L. V.; Simonsen, O.; Wernberg, O *Inorg. Chim. Acta* **1999**, *295*, 153. For other d^8 metal complexes of PSP ligands, see: (b) Morohashi, N.; Akahira, Y.; Tanaka, S.; Nishiyama, K.; Kajiwara, T.; Hattori, T. *Chem. Lett.* **2008**, *37*, 418.

(52) Xantphos-type ligands are typically cis κ^2(*PP*)-coordinated with the xanthene backbone adopting a butterfly conformation: (a) Kamer, P. C. J.; van Leeuwen, P. W. N. M.; Reek, J. N. H. *Acc. Chem. Res.* **2001**, *34*, 895. However, an approximately planar xanthene backbone has been observed in complexes where κ^3(*POP*)-coordination is favored: (b) Reference 48. (c) Sandee, A. J.; van der Veen, L. A.; Reek, J. N. H.; Kamer, P. C. J.; Lutz, M.; Spek, A. L.; van Leeuwen, P. W. N. M. *Angew. Chem., Int. Ed.* **1999**, *38*, 3231. (d) Nieczypor, P.; van Leeuwen, P. W. N. M.; Mol, J. C.; Lutz, M.; Spek, A. L. *J. Organomet. Chem.* **2001**, *625*, 58.

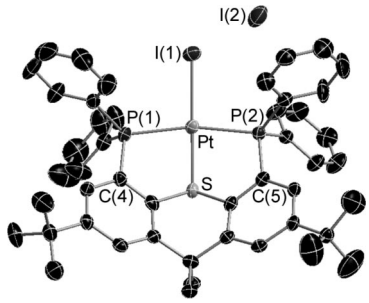

Figure 6. ORTEP of **10**·1.74CH_2Cl_2 with hydrogen atoms and solvent omitted for clarity (50% thermal ellipsoids). Selected bond lengths (Å) and angles (deg): Pt−P(1) 2.318(2), Pt−P(2) 2.310(2), Pt−S 2.252(2), Pt−I(1) 2.5824(6), Pt···I(2) 8.533(1), I(1)···I(2) 7.806(1), P(1)···P(2) 4.591(3), P(1)−Pt-S 83.75(6), P(2)−Pt-S 84.16(6), P(2)−Pt−I(1) 96.03(5), P1−Pt−I(1) 96.62(5), P(1)−Pt-P(2) 165.38(6), S−Pt−I(1) 175.95(4), ligand bend 46.96(24) [ligand bend = angle between the planes of the C4 ring and the C5 ring].

for complexes **9** and **10** confirms the steric accessibility of more traditional κ^3-coordination in 4,5-disubstituted thioxanthene ligands such as Thioxantphos and TXPB [involving a M−(η^1-BR_3) interaction in the case of TXPB], providing further evidence of an electronic origin for the observed M−{η^3(*BCC*)-BAr_3} interactions.

In summary, palladium (**2**) and nickel (**6**) complexes containing unambiguous examples of an η^3-bound arylborane were prepared, either by direct reaction of a zero-valent precursor with TXPB (in the case of nickel) or by stepwise reduction from a square planar dihalide complex (in the case of palladium). The short M−B bond lengths observed in **2** and **6**, combined with previously reported DFT calculations on a related rhodium complex (**1**), strongly suggest an electronic origin for the unusual η^3-arylborane coordination mode. This is further supported by observation of κ^3-coordination in platinum(II) Thioxantphos (the phosphorus-analogue of TXPB) complexes (**9** and **10**), which highlight the steric accessibility of bonding via three η^1-interactions in complexes of 4,5-disubstituted thioxanthene ligands such as TXPB. However, formation of η^1-coordinated arylborane complexes by reaction of [M(TXPB)] with dvds was prevented by facile displacement of the sulfur donor in the backbone of the TXPB ligand to form [(κ^1-TXPB)M(η^2:η^2-dvds)] {M = Pd (**7**) and M = Pt (**8**)}. Future work will focus on the oxidative addition reactivity of complexes **2** and **6**−**8** and their potential in C−C bond-forming catalysis.

Experimental Section

General Details. An argon-filled MBraun UNIlab glovebox equipped with a −30 °C freezer was employed for the manipulation and storage of all ligands and complexes,[53] and reactions were performed on a double-manifold high vacuum line using standard techniques.[54] Commonly utilized specialty glassware includes the swivel frit assembly, J-Young NMR tubes, and thick-walled flasks equipped with Teflon stopcocks. A Fisher Scientific Ultrasonic FS-30 bath was used to sonicate reaction mixtures where indicated, and in some cases, a Fischer Scientific Model 228 centrific centrifuge in combination with airtight Kimble-Kontes 15 mL conical centrifuge tubes was used to remove insoluble byproduct or to collect precipitated products. Residual oxygen and moisture were removed from the argon stream by passage through an Oxisorb-W scrubber from Matheson Gas Products. Anhydrous dme (1,2-dimethoxyethane) and CH_2Cl_2 were purchased from Aldrich. Hexanes and toluene were initially dried and distilled at atmospheric pressure from CaH_2 and sodium, respectively. Unless otherwise noted, all proteo solvents were stored over an appropriate drying agent (dme, toluene = Na/Ph_2CO; hexanes = Na/Ph_2CO/tetraglyme; CH_2Cl_2 = CaH_2) and introduced to reactions via vacuum transfer with condensation at −78 °C. Deuterated solvents (ACP Chemicals) were dried over CaH_2 (CD_2Cl_2, C_6D_5Br) or Na/Ph_2CO (C_6D_6, THF-d_8).

[$PdCl_2$(COD)], [$PtCl_2$(COD)], [PtI_2(COD)], [Ni(COD)$_2$], [Co_2], and Mg powder (325 mesh, 99%) were purchased from Strem Chemicals. [Pd_2(dba)$_3$], Ph_2PCl, 1,3-divinyltetramethyldisiloxane (dvds), *trans*,*trans*-dibenzylideneacetone (dba), Zn powder, $LiNEt_2$, and $LiN(SiMe_3)_2$ were purchased from Sigma-Aldrich. Prior to use, [$CoCp_2$] was sublimed, and Ph_2PCl, COD, COT, and dvds were distilled from molecular sieves. The compounds $TXBr_2$,[39] TXPB,[39] [Pd_2(dvds)$_3$],[46] [Pt(nb)$_3$],[55] and [Pt(COD)$_2$][55] were prepared according to the literature procedures. Note that in the literature preparation of [Pt(nb)$_3$], we found that 4−5 times the reported amount of OEt_2 was required to solubilize the Li_2[COT] reagent.

NMR spectroscopy (^{1}H, ^{13}C{^{1}H}, ^{11}B, ^{31}P, DEPT-135, COSY, HSQC, HMBC) was performed on Bruker DRX-500 and AV-600 spectrometers. All ^{1}H NMR and ^{13}C NMR spectra were referenced relative to $SiMe_4$ through a resonance of the employed deuterated solvent or proteo impurity of the solvent; C_6D_6 (δ 7.15 ppm), C_6D_5Br (δ 7.30, 7.02, 6.94 ppm), THF-d_8 (3.58, 1.73 ppm), and CD_2Cl_2 (5.32 ppm) for ^{1}H NMR and C_6D_6 (δ 128.0 ppm), C_6D_5Br (δ130.9, 129.3, 126.1, 122.3 ppm), THF-d_8 (67.57, 25.37 ppm), and CD_2Cl_2 (54.0 ppm) for ^{13}C NMR. ^{11}B and ^{31}P NMR spectra were referenced using an external standard of $BF_3(OEt_2)$ (0.0 ppm) and 85% H_3PO_4 in D_2O (0.0 ppm), respectively. Electrochemical studies were carried out using an PAR (Princeton Applied Research) Model 283 potentiostat (using PAR PowerCV software) in conjunction with a three-electrode cell under an argon atmosphere. The auxiliary electrode was a platinum wire, the pseudoreference electrode a silver wire, and the working electrode a platinum disk (1.6 mm diameter, Bioanalytical Systems). Solutions were 1×10^{-3} M in test compound and 0.1 M in [N-*n*-Bu_4][PF_6] as the supporting electrolyte. Under these conditions, values of $E_{1/2}$ (vs SCE) for the internal calibrant [$CoCp_2$][PF_6] are −0.90 and −2.04 V in THF.[56]

Combustion elemental analyses were performed on a Thermo EA1112 CHNS/O analyzer by Dr. Steve Kornic of this department. X-ray crystallographic analyses were performed on suitable crystals coated in Paratone oil and mounted on either (a) a P4 diffractometer with a Bruker Mo rotating-anode generator and a SMART1K CCD area detector or (b) a SMART APEX II diffractometer with a 3 kW Sealed tube Mo generator in the McMaster Analytical X-Ray (MAX) Diffraction Facility. One of the two molecules of hexane in **7**·2hexane, and both molecules of hexane in **6**·2hexane, were highly disordered and could not be modeled satisfactorily, so were treated using the SQUEEZE routine.[57] Herein, numbered proton and carbon atoms refer to the positions of the xanthene backbone in the TXPB or TXP_2 ligands (see Schemes 1 and 3).

[$PdCl_2$(TXPB)] (3). A solution of [$PdCl_2$(COD)] (125 mg, 4.37 $\times$ 10^{-4} mol) and TXPB (300 mg, 4.37 $\times$ 10^{-4} mol) in CH_2Cl_2 (15 mL) was stirred at room temperature for 1 h. The resulting brown-orange solution was evaporated to dryness in vacuo leaving an oily orange solid to which hexanes (20 mL) was added. After sonication for 1 h, the mixture was filtered to give an orange solid

(53) Degree of air sensitivity: Thioxantphos, **9** and **10** = low; TXPB, **3**-**5**, **7** and **8** = moderate; **1**, **2** and **6** = high.

(54) Burger, B. J.; Bercaw, J. E., Vacuum Line Techniques for Handling Air-Sensitive Organometallic Compounds. In *Experimental Organometallic Chemistry-A Practicum in Synthesis and Characterization*; American Chemical Society: Washington D.C., 1987; Vol. 357, p 79.

(55) Crascall, L. E.; Spencer, J. L. *Inorg. Synth.* **1990**, *28*, 126.

(56) Bard, A. J.; Garcia, E.; Kukharenko, S.; Strelets, V. V. *Inorg. Chem.* **1993**, *32*, 3528.

(57) Sluis, P. V. D.; Spek, A. L. *Acta Crystallogr.* **1990**, *A46*, 194.

which was washed with hexanes (×2) and dried in vacuo. Yield = 328 mg (87%). ^{1}H NMR (C_6D_5Br, 70 °C): δ 7.72 (broad s, 1H, C*H*^{1}), 7.60 (d, *J* 8 Hz, 4H, *o*-B*Ph*$_2$), 7.59 (broad s, 1H, C*H*^{8}), 7.50 (v broad s, 4H, *o*-P*Ph*$_2$), 7.47 (broad s, 1H, C*H*^{6}), 7.22 (t, *J* 7 Hz, 2H, *p*-P*Ph*$_2$), 7.14−7.08 (m, 9H, C*H*^{3} and *m*-P*Ph*$_2$ and *m*-B*Ph*$_2$), 7.06 (d, *J* 7 Hz, 2H, *p*-B*Ph*$_2$), 1.69 (broad s, 6H, C*Me*$_2$), 1.15 (s, 9H, C^{7}C*Me*$_3$), 1.07 (s, 9H, C^{2}C*Me*$_3$). ^{13}C{^{1}H} NMR (C_6D_5Br, 70 °C): δ 153.90 (s, *C*^{2}CMe$_3$), 151.9 (broad s, *C*^{5}), 150.8 (broad s, *ipso*-B*Ph*$_2$), 150.61 (s, *C*^{7}CMe$_3$), 145.75 (d, *J* 14 Hz, *C*^{10}), 139.55 (s, *C*^{13}), 136.02 (d, *J* 19 Hz, *C*^{11}), 135.00 (s, *o*-B*Ph*$_2$), 133.89 (s, *C*H^6), 133.85 (d, *J* 12 Hz, *o*-P*Ph*$_2$), 132.11 (s, *p*-P*Ph*$_2$), 128.73 (s, *C*H^3), 128.67 (d, *J* 13 Hz, *m*-P*Ph*$_2$), 127.38 (d, *J* 62 Hz, *C*^{4} or *ipso*-P*Ph*$_2$), 126.82 (s, *m*-B*Ph*$_2$), 126.68 (s, *C*^{12}), 126.07 (s, *C*H^1), 125.80 (s, *p*-B*Ph*$_2$), 120.08 (s, *C*H^8), 42.14 (s, *C*Me$_2$), 34.87 (s, 2 × C^2*C*Me$_3$), 34.70 (s, 2 × C^7*C*Me$_3$), 31.08 (s, C^{7}C*Me*$_3$), 30.80 (s, C^{2}C*Me*$_3$), 26.85 (broad s, C*Me*$_2$). ^{31}P{^{1}H} (CD_2Cl_2): δ 58.42 (s). ^{11}B (CD_2Cl_2): δ 12.9 (broad s). Anal. Calcd for $C_{47}H_{48}PSBCl_2Pd$: C, 65.33; H, 5.60. Found: C, 65.33; H, 5.57.

[{PdCl(TXPB)}$_2$] (4). A solution of [Pd(dba)(TXPB)]·CH_2Cl_2 (**5**) (80 mg, 7.19 × 10^{-5} mol) and [$PdCl_2$(TXPB)] (**3**) (62 mg, 7.19 × 10^{-5} mol) in CH_2Cl_2 (4 mL) was heated in a sealed flask at 50 °C for 2 days. The resulting bright red solution was then layered with hexanes and cooled to −30 °C. After several days, the orange-brown mother liquors were decanted to leave red crystals which were dried in vacuo. Yield = 60 mg (50%). X-ray quality crystals of **4**·hexane were grown from CH_2Cl_2/hexane at −30 °C. ^{1}H NMR (CD_2Cl_2): δ 7.81 (dd, *J* 12, 8 Hz, 2H, *o*-P*Ph*$_2$ B), 7.58 (s, 1H, C*H*^{1}), 7.53 (d, *J* 2 Hz, 1H, C*H*^{8}), 7.51 (td, *J* 7, 2 Hz, 1H, *p*-P*Ph*$_2$ A), 7.40 (app td, *J* 7, 2 Hz, 2H, *m*-P*Ph*$_2$ A), 7.2−7.1 (m, 10H, B*Ph*$_2$), 7.15 (s, 1H, C*H*^{3}), 7.12 (d, *J* 2 Hz, C*H*^{6}), 7.07 (dd, *J* 12, 8 Hz, 2H, *o*-P*Ph*$_2$ B), 6.45 (t, *J* 7 Hz, 1H, *p*-P*Ph*$_2$ B), 5.95 (t, *J* 6 Hz, 2H, *m*-P*Ph*$_2$ B), 2.05 (s, 3H, C*Me*$_2$), 1.25 (s, 9H, C^{2}C*Me*$_3$), 1.23 (s, 9H, C^{7}C*Me*$_3$), 0.99 (s, 3H, C*Me*$_2$). ^{13}C{^{1}H} NMR (CD_2Cl_2): δ 153.24, 152.84 (broad s, 2 × *ipso*-B*Ph*$_2$), 151.10 (s, *C*^{2}CMe$_3$), 150.08 (broad s, *C*^{5}), 149.24 (s, *C*^{7}CMe$_3$), 144.72 (d, *J* 11 Hz, *C*^{10}), 140.20 (s, *C*^{13}), 136.71 (d, *J* 20 Hz, *C*^{11}), 136.29 (d, *J* 14 Hz, *o*-P*Ph*$_2$ A), 135.17 (d, *J* 47 Hz, *C*^{4}), 134.87, 134.72, 127.56, 125.76, 125.47 (5 × s, B*Ph*$_2$), 133.43 (s, *C*H^6), 133.04 (d, *J* 9 Hz, *o*-P*Ph*$_2$ B), 131.62 (s, *p*-P*Ph*$_2$ A), 131.45 (d, *J* 55 Hz, *ipso*-P*Ph*$_2$), 130.86 (d, *J* 57 Hz, *ipso*-P*Ph*$_2$), 129.31 (s, *C*^{12}), 129.15 (s, *p*-P*Ph*$_2$ B), 129.01 (d, 11 Hz, *m*-P*Ph*$_2$ A), 127.2 (*C*H^3), 127.02 (s, *m*-P*Ph*$_2$ B), 123.84 (s, *C*H^1), 120.08 (s, *C*H^8), 41.58 (s, *C*Me$_2$), 35.59 (s, C^2*C*Me$_3$), 35.32 (s, C^7*C*Me$_3$), 31.76 (s, *C*^{7}C*Me*$_3$), 31.52 (s, C^{2}C*Me*$_3$), 28.40, 25.76 (s, C*Me*$_2$). ^{31}P{^{1}H} (CD_2Cl_2): δ 36.47 (s). ^{11}B (CD_2Cl_2): δ 2 (broad s). Anal. Calcd for $C_{94}H_{96}P_2S_2B_2Cl_2Pd_2$: C, 68.13; H, 5.84. Found: C, 67.94; H, 5.96.

[Pd(TXPB)] (2). A mixture of [$PdCl_2$(TXPB)] (**3**; 200 mg, 2.31 × 10^{-4} mol) and Mg powder (100 mg, 4.17 mmol) in THF (10 mL) was sonicated for 30 min at room temperature and then stirred vigorously for 10 min, resulting in a color change from bright orange-yellow to orange-red. This process was then repeated resulting in a color change to deep red, and then to yellow-brown. The mixture was then evaporated to dryness in vacuo, dissolved in hexanes (5 mL) and filtered through a short column of celite. The supernatant was evaporated to dryness to yield **2** as a yellow-brown powder (yield 116 mg, 63%). X-ray quality crystals of **2**·toluene were grown from toluene at −30 °C. ^{1}H NMR (THF-d_8, −30 °C): δ 7.63 (app t, *J* 7 Hz, 1H, *m*(2)-B*Ph*$_2$ A), 7.58 (s, 1H, C*H*^{1}), 7.49 (s, 1H, C*H*^{8}), 7.48 (m, 2H, *o*-B*Ph*$_2$ B), 7.42 (s, 1H, C*H*^{6}), 7.37 (m, 10H, P*Ph*$_2$ B), 7.29 (t, *J* 7 Hz, 1H, *p*-P*Ph*$_2$ A), 7.22 (t, *J* 7 Hz, 2H, *m*-P*Ph*$_2$ A), 7.13 (d, *J* 7 Hz, 1H, *p*-B*Ph*$_2$ B), 7.12 (t, *J* 7 Hz, 2H, *m*-B*Ph*$_2$ B), 7.04 (t, *J* 7 Hz, 1H, *p*(3)-B*Ph*$_2$ A), 7.03 (app t, *J* 7 Hz, 1H, *m*(4)-B*Ph*$_2$ A), 6.83 (d, *J* 6 Hz, 1H, C*H*^{3}), 6.62 (d, *J* 7 Hz, 1H, *o*(1)-B*Ph*$_2$ A), 6.53 (d, *J* 7 Hz, 1H, *o*(5)-B*Ph*$_2$ A), 6.45 (dd, *J* 11, 7 Hz, 2H, *o*-P*Ph*$_2$), 2.09, 1.71 (s, 2 × 3H, C*Me*$_2$), 1.37, 1.05 (s, 2 × 9H, C*Me*$_3$).[58] ^{13}C{^{1}H} NMR (THF-d_8, −30 °C): δ 151.34 (s, *C*^{7}CMe$_3$), 151.27 (broad s, *C*^{5}), 151.07 (s, *C*^{2}CMe$_3$), 147.49 (broad s, *ipso*-B*Ph*$_2$ B), 145.33 (d, *J* 6 Hz, *C*^{10}), 143.38 (s, *C*^{13}), 142.16 (d, *J* 15 Hz, *C*^{12}), 140.19 (d, *J* 44 Hz, *C*^{11}), 138.21 (d, *J* 38 Hz, *C*^{4}), 135.60 (s, *o*-B*Ph*$_2$ B), 135.52 (d, *J* 40 Hz, *ipso*-P*Ph*$_2$ A and B), 134.86 (s, *m*(2)-B*Ph*$_2$ A), 134.56 (d, *J* 19 Hz, *o*-P*Ph*$_2$ A), 133.65 (d, *J* 16 Hz, *o*-P*Ph*$_2$ B), 132.50 (s, *o*(5)-B*Ph*$_2$ A), 130.68 (s, *p*-P*Ph*$_2$ A), 130.38 (s, *p*-P*Ph*$_2$ B), 129.94 (d, *C*H^3), 129.9 (d, *m*-P*Ph*$_2$ B), 128.93 (d, *J* 10 Hz, *m*-P*Ph*$_2$ A), 128.57 (s, *p*(3)-B*Ph*$_2$ A), 128.38 (s, *p*-B*Ph*$_2$ B), 127.68 (s, *m*-B*Ph*$_2$ B), 127.44 (s, *C*H^6), 125.30 (d, *J* 9 Hz, *m*(4)-B*Ph*$_2$ A), 124.61 (s, *C*H^1), 120.41 (s, *C*H^8), 115.63 (broad s, *ipso*-B*Ph*$_2$ A), 101.05 (s, *o*(1)-B*Ph*$_2$ A), 43.43 (s, *C*Me$_2$), 35.86, 35.70 (2 × s, *C*Me$_3$), 32.24, 31.49 (2 × s, C*Me*$_3$), 26.35, 25.94 (2 × s, C*Me*$_2$).[58] ^{31}P{^{1}H} (C_6D_6): δ 17.99 (s). ^{11}B (C_6D_6): δ 31 (broad s).[59] Anal. Calcd for $C_{47}H_{48}PSBPd$: C, 71.17; H, 6.10. Found: C, 70.53; H, 6.47.

[Ni(TXPB)]·0.5hexane (6). A mixture of [Ni(COD)$_2$] (40 mg, 1.46 × 10^{-4} mol) and TXPB (100 mg, 1.46 × 10^{-4} mol) in toluene (5 mL) was stirred for 2 h at room temperature. The resulting dark red-orange solution was then evaporated to dryness, sonicated in hexanes (5 mL), and filtered to collect a brick red solid which was washed with hexanes (×2) and dried in vacuuo. Yield 80 mg (70%). In several instances, this product contained an impurity with ^{31}P NMR δ 42 ppm. However, this impurity could be removed by crystallization from dme/hexanes at −30 °C. X-ray quality crystals of **6**·2hexane were also grown from dme/hexane at −30 °C. ^{1}H NMR (THF-d_8, −30 °C): δ 7.65 (m, 2H, *o*-P*Ph*$_2$ A), 7.57 (s, 1H, C*H*^{1}), 7.48 (s, 1H, C*H*^{8}), 7.46 (s, 1H, C*H*^{6}), 7.44 (m, 3H, *m*- and *p*-P*Ph*$_2$ A), 7.41 (d, *J* 7 Hz, 2H, *o*-B*Ph*$_2$ B), 7.26 (app t, *J* 7 Hz, 1H, *m*(2)-B*Ph*$_2$ A), 7.25 (t, *J* 7 Hz, 1H, *p*-P*Ph*$_2$ B), 7.20 (app t, *J* 7 Hz, 2H, *m*-P*Ph*$_2$ B), 7.09 (t, *J* 7 Hz, 1H, *p*-B*Ph*$_2$ B), 7.07 (app t, *J* 7 Hz, 2H, *m*-B*Ph*$_2$ B), 6.94 (d, *J* 6 Hz, 1H, C*H*^{3}), 6.63 (app t, *J* 7 Hz, 1H, *m*(4)-B*Ph*$_2$ A), 6.44 (dd, *J* 10, 7 Hz, 2H, *o*-P*Ph*$_2$ B), 6.30 (d, *J* 7 Hz, 1H, *o*(5)-B*Ph*$_2$ A), 6.26 (t, *J* 7 Hz, 1H, *p*(3)-B*Ph*$_2$ A), 5.68 (d, *J* 7 Hz, 1H, *o*(1)-B*Ph*$_2$ A), 2.07, 1.62 (s, 2 × 3H, C*Me*$_2$), 1.37, 1.12 (s, 2 × 9H, C*Me*$_3$).[58] ^{13}C{^{1}H} NMR (THF-d_8, −30 °C): δ 152.11 (broad s, *C*^{5}), 151.39, 151.24 (s, *C*^{2}CMe$_3$, *C*^{7}CMe$_3$), 148.59 (broad s, *ipso*-B*Ph*$_2$ B), 144.26 (d, *J* 8 Hz, *C*^{10}), 142.50 (d, *J* 37 Hz, *C*^{11}), 142.11 (s, *C*^{13}), 141.90 (d, *J* 15 Hz, *C*^{12}), 138.61 (d, *J* 43 Hz, *C*^{4}), 137.54 (s, *m*(2)-B*Ph*$_2$ A), 135.07 (s, *o*-B*Ph*$_2$ B), 134.64 (d, *J* 16 Hz, *o*-P*Ph*$_2$ A), 133.93 (d, *J* 32 Hz, *ipso*-P*Ph*$_2$ A), 133.63 (d, *J* 14 Hz, *o*-P*Ph*$_2$ B), 131.46 (d, *J* 31 Hz, *ipso*-P*Ph*$_2$ B), 131.16 (s, *p*-P*Ph*$_2$ A), 130.58 (s, *o*(5)-B*Ph*$_2$ A), 130.10 (d, *J* 9 Hz, *m*-P*Ph*$_2$ A), 129.92 (s, *p*-P*Ph*$_2$ B), 129.76 (d, *J* 9 Hz, *m*(4)-B*Ph*$_2$ A), 128.8 (d, *C*H^3), 128.7 (d, *m*-P*Ph*$_2$ B), 128.37 (s, *m*-B*Ph*$_2$ B), 127.10 (s, *p*-B*Ph*$_2$ B), 126.91 (s, *C*H^8), 124.74 s, *C*H^1), 123.70 (s, *p*(3)-B*Ph*$_2$ A), 120.47 (s, *C*H^6), 105.36 (broad s, *ipso*-B*Ph*$_2$ A), 91.37 (s, *o*(1)-B*Ph*$_2$ A), 42.94 (s, *C*Me$_2$), 35.94, 35.80 (2 × s, *C*Me$_3$), 32.34, 31.59 (2 × s, C*Me*$_3$), 27.06, 25.00 (2 × s, C*Me*$_2$).[58] ^{31}P{^{1}H} (C_6D_6): δ 33.86 (s). ^{11}B (C_6D_6): δ 30 (broad s).[59] Anal. Calcd for $C_{50}H_{55}PSBNi$: C, 76.16; H, 7.03. Found: C, 75.89; H, 7.31.

[(κ^1-TXPB)Pd(η^2:η^2-dvds)] (7). A solution of TXPB (100 mg, 1.46 × 10^{-4} mol) in hexanes (0.8 mL) was added to a solution of [Pd_2(dvds)$_3$] (56 mg, 7.25 × 10^{-5} mol) in hexanes (0.7 mL) followed by stirring for 5 min before filtration through a short (0.3 × 1 cm) plug of Celite and elution with hexanes (2 × 0.5 mL). The resulting orange-brown solution was cooled to −30 °C to yield a beige-yellow semicrystalline solid. The mother liquors were removed from the solid at −30 °C before warming to room temperature, at which point the solid partially dissolved as a result of liberated lattice solvent. The resulting yellow-orange mixture was dried in vacuo to yield **7** as a beige solid. Yield = 112 mg (79%). X-ray quality crystals of **7**·hexane were grown from hexane

(58) The metal-coordinated *B*-phenyl ring is labeled *A* and is numbered to indicate the position of each carbon and proton relative to the coordinated ortho position. For example, the coordinated ortho position is labeled "*o*(1)-B*Ph*$_2$ A", while the adjacent meta position is labeled "*m*(2)-B*Ph*$_2$ A".

(59) Complex **2** (THF-d_8): ^{31}P δ 19.12 ppm (s), ^{11}B δ 30 ppm (broad s). Complex **6** (THF-d_8): ^{31}P δ 34.37 ppm (s), ^{11}B δ 28 ppm (broad s).

at −30 °C and mounted without warming above −20 °C to prevent solvent loss. ^{1}H NMR (C_6D_6): δ 7.73 (s, 1H, C*H*^{8}), 7.70 (s, 1H, C*H*^{1}), 7.63 (d, *J* 7 Hz, 4H, *o*-B*Ph*$_2$), 7.48 (m, 4H, *o*-P*Ph*$_2$), 7.29 (t, *J* 7 Hz, 2H, *p*-B*Ph*$_2$), 7.28 (s, 1H, C*H*^{6}), 7.21 (app t, *J* 7 Hz, 4H, *m*-B*Ph*$_2$), 7.16 (d, 1H, C*H*^{3}), 6.90 (m, 6H, *m*- and *p*-P*Ph*$_2$), 3.36 (dd, $^3J_{H,H}$ 16 Hz, $^3J_{H,P}$ 5 Hz, 2H, CH═C*H*$_2$), 3.32 (dd, $^3J_{H,H}$ 12 Hz, $^3J_{H,P}$ 6 Hz, 2H, CH═C*H*$_2$), 3.08 (ddd, $^3J_{H,H}$ 16, 12 Hz, $^3J_{H,P}$ 5 Hz, 2H, C*H*═CH$_2$), 1.82 (s, 6H, C*Me*$_2$), 1.21 (s, 9H, C^{7}C*Me*$_3$), 1.17 (s, 9H, C^{2}C*Me*$_3$), 0.48, −0.05 (s, 2 × 6H, Si*Me*$_2$). ^{13}C{^{1}H} NMR (C_6D_6): δ 148.47 (s, *C*^{2}CMe$_3$), 148.23 (s, *C*^{7}CMe$_3$), 144.38 (broad s, *C*^{5}), 143.22 (s, *C*^{10}), 142.53 (broad s, *ipso*-B*Ph*$_2$), 141.88 (s, *C*^{13}), 139.13 (s, *o*-B*Ph*$_2$), 136.48 (d, *J* 17 Hz, *C*^{11}), 136.28 (d, *J* 28 Hz, *ipso*-P*Ph*$_2$), 135.77 (d, *J* 30 Hz, *C*^{4}), 135.20 (s, *C*^{12}), 134.57 (d, *J* 15 Hz, *o*-P*Ph*$_2$), 132.15 (s, *p*-B*Ph*$_2$), 130.30 (s, *C*H^6), 129.35 (s, *p*-P*Ph*$_2$), 128.29 (d, *J* 9 Hz, *m*-P*Ph*$_2$), 127.93 (s, *m*-B*Ph*$_2$), 126.99 (s, *C*H^3), 122.32 (s, *C*H^8), 121.86 (s, *C*H^1), 69.64 (s, CH═*C*H$_2$), 67.98 (d, $^2J_{C,P}$ 7 Hz, *C*H═CH$_2$), 41.21 (s, *C*Me$_2$), 35.02 (s, C^2*C*Me$_3$), 34.83 (s, C^7*C*Me$_3$), 31.53 (s, C^{7}C*Me*$_3$), 31.40 (s, C^{2}C*Me*$_3$), 25.33 (s, C*Me*$_2$), 1.91, −1.05 (2 × s, Si*Me*$_2$). ^{31}P{^{1}H} (C_6D_6): δ 23.8 (s). ^{11}B (C_6D_6): δ 74 (broad s). Anal. Calcd for $C_{55}H_{66}OPSBSi_2Pd$: C, 67.44; H, 6.79. Found: C, 67.59; H, 6.99.

[(κ^1-TXPB)Pt(η^2:η^2-dvds)]·hexane (8). A solution of dvds (34 mg, 3.13 × 10^{-4} mol) in hexanes (1 mL) was added to a solution of [Pt(COD)$_2$] (68 mg, 1.65 × 10^{-4} mol) in hexanes (1 mL). The resulting mixture was stirred for 5 min and filtered to give a pale brown solution, to which a solution of TXPB (113 mg, 1.65 × 10^{-4} mol) in hexanes (1 mL) was added. After being stirred for 5 min, the pale brown solution was filtered and cooled to −30 °C to yield a pale-fawn solid which was dried in vacuo. Yield = 112 mg (59%). ^{1}H NMR (C_6D_6): δ 7.73 (d, *J* 2 Hz, 1H, C*H*^{8}), 7.70 (s, 1H, C*H*^{1}), 7.63 (d, *J* 7 Hz, 4H, *o*-B*Ph*$_2$), 7.49 (m, 4H, *o*-P*Ph*$_2$), 7.29 (t, *J* 7 Hz, 2H, *p*-B*Ph*$_2$), 7.28 (s, 1H, C*H*^{6}), 7.24 (d, *J* 11 Hz, 1H, C*H*^{3}), 7.20 (app t, *J* 7 Hz, 4H, *m*-B*Ph*$_2$), 6.88 (m, 6H, *m*- and *p*-P*Ph*$_2$), 2.49 (dd, $^3J_{H,H}$ 14 Hz, $^3J_{H,P}$ 7 Hz, 2H, CH═C*H*$_2$), 2.49 (dd, $^3J_{H,H}$ 12 Hz, $^3J_{H,P}$ 7 Hz, 2H, CH═C*H*$_2$), 2.49 (ddd, $^3J_{H,H}$ 14, 12 Hz, $^3J_{H,P}$ 7 Hz, 2H, C*H*═CH$_2$), 1.80 (s, 6H, C*Me*$_2$), 1.21 (s, 9H, C^{7}C*Me*$_3$), 1.17 (s, 9H, C^{2}C*Me*$_3$), 0.55, −0.08 (s, 2 × 6H, Si*Me*$_2$). ^{13}C{^{1}H} NMR (C_6D_6): δ 148.21 (s, 2 × *C*CMe$_3$), 144.31 (broad s, *C*^{5}), 143.50 (d, *J* 7 Hz, *C*^{10}), 142.61 (broad s, *ipso*-B*Ph*$_2$), 141.94 (s, *C*^{13}), 139.11 (s, *o*-B*Ph*$_2$), 136.77 (d, *J* 12 Hz, *C*^{11}), 135.23 (d, *J* 45 Hz, *ipso*-P*Ph*$_2$), 135.18 (s, *C*^{12}), 134.8 (d, *C*^{4}), 134.49 (d, *J* 12 Hz, *o*-P*Ph*$_2$), 132.12 (s, *p*-B*Ph*$_2$), 130.56 (s, *C*H^6), 129.63 (s, *p*-P*Ph*$_2$), 128.08 (d, *J* 10 Hz, *m*-P*Ph*$_2$), 127.88 (s, *m*-B*Ph*$_2$), 127.5 (s, *C*H^3), 122.31 (s, *C*H^1 and *C*H^8), 52.32 (s, $^1J_{C,Pt}$ 162 Hz, CH═*C*H$_2$), 46.56 (d, $^2J_{C,P}$ 11 Hz, $^1J_{C,Pt}$ 117 Hz, *C*H═CH$_2$), 41.28 (s, *C*Me$_2$), 35.02 (s, C^2*C*Me$_3$), 34.83 (s, C^7*C*Me$_3$), 31.51 (s, C^{7}C*Me*$_3$), 31.36 (s, C^{2}C*Me*$_3$), 25.24 (s, C*Me*$_2$), 1.83, −1.63 (2 × s, Si*Me*$_2$). ^{31}P{^{1}H} (**C$_6$D$_6$**): δ 21.1 (s, $J_{^{31}P,^{195}Pt}$ 3361 Hz). ^{11}B (C_6D_6): δ 74 (broad s). Anal. Calcd for $C_{61}H_{80}OPSBSi_2Pt$: C, 63.14; H, 6.95. Found: C, 63.36; H, 6.43.

2,7-Di-*tert*-butyl-4,5-bis(diphenylphosphino)-9,9-dimethylthioxanthene (TXP$_2$). A 2.0 M solution of *n*-butyllithium (2.1 mL, 4.13 mmol) was added to a solution of ^{t}Bu$_2$TXBr$_2$ (1.0 g, 2.01 mmol) in toluene (80 mL) at −78 °C. The mixture was then allowed to warm to room temperature over several hours and stirred for a further 12 h. After the mixture was cooled to −78 °C, Ph_2PCl (0.74 mL, 4.13 mmol) was added, and the solution was allowed to warm to room temperature, stirred for a further 12 h, filtered, and evaporated to dryness in vacuo to give a slightly oily white solid. This was slurried in hexanes (50 mL), sonicated, cooled to −78 °C, and then filtered to collect a white solid which was dried in vacuo. Yield = 960 mg (67%). ^{1}H NMR (**CD$_2$Cl$_2$**): δ 7.54 (d, $^4J_{H,H}$ 1 Hz, 2H, C*H*^{1}), 7.40−7.30 (m, 20H, P*Ph*$_2$), 6.78 (dd, *J* = 4, 1 Hz, 2H, C*H*^{3}), 1.73 (s, 6H, C*Me*$_2$), 1.15 (s, 18H, C*Me*$_3$). ^{13}C{^{1}H} NMR (CD_2Cl_2): δ 149.62 (s, *C*^{2}CMe$_3$), 143.22 (s, *C*^{10}), 137.50 (d, *J* 12 Hz, *ipso*-P*Ph*$_2$), 136.31 (d, *J* 9 Hz, *C*^{4}), 136.13 (d, *J* 10 Hz, *C*^{11}), 134.58 (d, *J* 20 Hz, *ortho*-P*Ph*$_2$), 129.1 (d, *m*-P*Ph*$_2$), 129.0 (s, *p*-P*Ph*$_2$), 128.78 (s, *C*H^3), 122.44 (s, *C*H^1), 41.71 (s, *C*Me$_2$), 35.31 (s, *C*Me$_3$), 31.52 (s, C*Me*$_3$), 25.34 (s, C*Me*$_2$). ^{31}P{^{1}H} (**CD$_2$Cl$_2$**): δ −10.01 (s). Anal. Calcd for $C_{47}H_{48}P_2S$: C, 79.86; H, 6.84. Found: C, 79.57; H, 6.59.

[PtCl$_2$(TXP$_2$)]·CH$_2$Cl$_2$ (9). A solution of [PtCl$_2$(COD)] (132 mg, 3.54 × 10^{-4} mol) and TXP$_2$ (250 mg, 3.54 × 10^{-4} mol) in CH_2Cl_2 (25 mL) was stirred at room temperature for 1 h. The resulting pale yellow solution was evaporated to lower volume (10 mL) in vacuo, and hexanes (15 mL) was added. The mixture was then filtered to collect a white solid which was washed with hexanes and dried in vacuo. Yield = 245 mg (66%). ^{1}H NMR (CD_2Cl_2): δ 7.86 (app quart., *J* 7 Hz, 4H, *o*-P*Ph*$_2$ A), 7.85 (m, 2H, C*H*^{1}), 7.73 (app t, *J* 7 Hz, 2H, *p*-P*Ph*$_2$ A), 7.69 (app t, *J* 8 Hz, 4H, *m*-P*Ph*$_2$ A), 7.61 (app t, *J* 8 Hz, 2H, *p*-P*Ph*$_2$ B), 7.50 (app t, *J* 7 Hz, 4H, *m*-P*Ph*$_2$ B), 7.41 (app quart, *J* 7 Hz, 4H, *o*-P*Ph*$_2$ B), 7.37 (app td, *J* 5, 1.6 Hz, 2H, C*H*^{3}), 2.22, 1.56 (s, 2 × 3H, C*Me*$_2$), 1.28 (s, 18H, C*Me*$_3$). ^{13}C{^{1}H} NMR (CD_2Cl_2): δ 157.41 (s, *C*^{2}CMe$_3$), 144.66 (s, *C*^{10}), 134.48 (app t, *J* 15 Hz, *C*^{11}), 134.22 (app t, *J* 6 Hz, *o*-P*Ph*$_2$ B), 134.03 (app t, *J* 7 Hz, *o*-P*Ph*$_2$ A), 133.80 (s, *p*-P*Ph*$_2$ A), 133.54 (s, *p*-P*Ph*$_2$ B), 132.79 (app t, *J* 29 Hz, *C*^{4}), 131.23 (s, *C*H^3), 130.66 (app t, *J* 5 Hz, *m*-P*Ph*$_2$ A), 129.73 (app t, *J* 5 Hz, *m*-P*Ph*$_2$ B), 128.06 (s, *C*H^1), 126.74 (app t, *J* 29 Hz, *ipso*-P*Ph*$_2$ A), 125.27 (app t, *J* 32 Hz, *ipso*-P*Ph*$_2$ B), 44.00 (s, *C*Me$_2$), 36.11 (s, *C*Me$_3$), 31.39 (s, C*Me*$_3$), 28.30, 24.91 (s, C*Me*$_2$). ^{31}P{^{1}H} (CD_2Cl_2): δ 41.46 (s, $^1J_{31P,195Pt}$ 2429 Hz). Anal. Calcd for $C_{48}H_{50}P_2SCl_4Pt$: C, 54.50; H, 4.76. Found: C, 54.80; H, 4.64.

[PtI$_2$(TXP$_2$)]·1.5toluene (10). A mixture of [PtI$_2$(COD)] (70 mg, 1.26 × 10^{-4} mol) and TXP$_2$ (93 mg, 1.32 × 10^{-4} mol) in toluene (4 mL) was stirred at room temperature for 2 h. The resulting mixture was centrifuged, and the yellow mother liquors removed to collect a bright yellow powder. Toluene (3 mL) was again added, and the mixture was stirred and then centrifuged before removal of the nearly colorless mother liquors. The resulting bright yellow powder was dried in vacuo. Yield = 122 mg (72%). X-ray quality crystals of **4**·1.74CH_2Cl_2 were grown from CH_2Cl_2/hexane at −30 °C. ^{1}H NMR (CD_2Cl_2): δ 7.94 (app quart., *J* 7 Hz, 4H, *o*-P*Ph*$_2$ A), 7.85 (s, 2H, C*H*^{1}), 7.73 (app t, *J* 7 Hz, 2H, *p*-P*Ph*$_2$ A), 7.68 (app t, *J* 7 Hz, 4H, *m*-P*Ph*$_2$ A), 7.58 (app t, *J* 7 Hz, 2H, *p*-P*Ph*$_2$ B), 7.49 (app t, *J* 7 Hz, 4H, *m*-P*Ph*$_2$ B), 7.32 (app quart., *J* 7 Hz, 4H, *o*-P*Ph*$_2$ B), 7.29 (t, *J* 5 Hz, 2H, C*H*^{3}), 2.23, 1.58 (s, 2 × 3H, C*Me*$_2$), 1.28 (s, 18H, C*Me*$_3$). ^{13}C{^{1}H} NMR (CD_2Cl_2) δ 157.29 (s, *C*^{2}CMe$_3$), 144.51 (s, *C*^{10}), 134.64 (app t, *J* 7 Hz, o-P*Ph*$_2$ A), 134.38 (app t, *J* 6 Hz, *o*-P*Ph*$_2$ B), 134 (*C*^{11}), 133.82 (s, *p*-P*Ph*$_2$ A), 133.42 (s, *p*-P*Ph*$_2$ B), 131.75 (s, *C*H^3), 130.69 (app t, *J* 5 Hz, *m*-P*Ph*$_2$ A), 129.38 (app t, *J* 5 Hz, *m*-P*Ph*$_2$ B), 127.93 (s, *C*H^1), 127.58 (app t, *J* 33 Hz, *ipso*-PPh$_2$ B), 127.04 (app t, *J* 29 Hz, *ipso*-PPh$_2$ B), 44.02 (s, *C*Me$_2$), 36.15 (s, *C*Me$_3$), 31.46 (s, C*Me*$_3$), 28.35, 25.09 (s, C*Me*$_2$). ^{31}P{^{1}H} (CD_2Cl_2): δ 38.64 (s, $^1J_{31P,195Pt}$ 2383 Hz). Anal. Calcd for $C_{57.5}H_{60}P_2SI_2Pt$: C, 53.36; H, 4.67. Found: C, 53.45; H, 4.65.

Acknowledgment. Funding for this work was provided to D.J.H.E. as a McMaster University Start-Up fund, an NSERC of Canada Discovery Grant, and CFI and OIT New Opportunities Grants.

Supporting Information Available: X-ray crystallographic data in PDF and CIF format. This material is available free of charge via the Internet at http://pubs.acs.org.

OM800670E